



HAL
open science

A novel toxic effect of foodborne trichothecenes: The exacerbation of genotoxicity

Marion Garofalo, Delphine Payros, Marie Penary, Eric Oswald, Jean-Philippe Nougayrède, Isabelle Oswald

► **To cite this version:**

Marion Garofalo, Delphine Payros, Marie Penary, Eric Oswald, Jean-Philippe Nougayrède, et al.. A novel toxic effect of foodborne trichothecenes: The exacerbation of genotoxicity. *Environmental Pollution*, 2023, 317, pp.120625. 10.1016/j.envpol.2022.120625 . hal-03885045

HAL Id: hal-03885045

<https://hal.inrae.fr/hal-03885045>

Submitted on 1 Jun 2023

HAL is a multi-disciplinary open access archive for the deposit and dissemination of scientific research documents, whether they are published or not. The documents may come from teaching and research institutions in France or abroad, or from public or private research centers.

L'archive ouverte pluridisciplinaire **HAL**, est destinée au dépôt et à la diffusion de documents scientifiques de niveau recherche, publiés ou non, émanant des établissements d'enseignement et de recherche français ou étrangers, des laboratoires publics ou privés.

Copyright

1 **A novel toxic effect of foodborne trichothecenes: the exacerbation of genotoxicity**

2

3 Marion Garofalo^{a,b}, Delphine Payros^{a,b}, Marie Penary^b, Eric Oswald^{b,c}, Jean-Philippe
4 Nougayrède^{b,T}, Isabelle P. Oswald^{a,T*}.

5

6 ^aToxalim (Research Centre in Food Toxicology), Université de Toulouse, INRAE, ENVT, INP-
7 Purpan, UPS, Toulouse, France

8 ^bIRSD, Université de Toulouse, INSERM, INRAE, ENVT, UPS, Toulouse, France

9 ^cCHU Toulouse, Hôpital Purpan, Service de Bactériologie-Hygiène, Toulouse, France

10

11 ^TCo senior author

12 *Corresponding authors: isabelle.oswald@inrae.fr;

13 Keywords: trichothecenes; genotoxins; colibactin; DNA damage.

14

15 **ABSTRACT**

16 Trichothecenes (TCTs) are very common mycotoxins. While the effects of DON, the most
17 prevalent TCT, have been extensively studied, less is known about the effect of other TCTs.
18 DON has ribotoxic, pro-inflammatory, and cytotoxic potential and induces multiple toxic
19 effects in humans and animals. Although DON is not genotoxic by itself, it has recently been
20 shown that this toxin exacerbates the genotoxicity induced by model or bacterial genotoxins.
21 Here, we show that five TCTs, namely T-2 toxin (T-2), diacetoxyscirpenol (DAS), nivalenol
22 (NIV), fusarenon-X (FX), and the newly discovered NX toxin, also exacerbated the DNA
23 damage inflicted by various genotoxins. The exacerbation was dose dependent and observed
24 with phleomycin, a model genotoxin, captan, a pesticide with genotoxic potential, and
25 colibactin, a bacterial genotoxin produced by the intestinal microbiota. For this newly described
26 effect, the TCTs ranked in the following order: T-2>DAS>FX>NIV≥DON≥NX. The genotoxic
27 exacerbating effect of TCTs correlated with their ribotoxic potential, as measured by inhibition
28 of protein synthesis. In conclusion, our data demonstrate that TCTs, which are not genotoxic
29 by themselves, exacerbate DNA damage induced by various genotoxins. Therefore, foodborne
30 TCTs could enhance the carcinogenic potential of genotoxins present in the diet or produced
31 by intestinal bacteria.

32

33 **KEY WORDS**

34 mycotoxins, pesticides, microbiota, colibactin, carcinogenic potential

35

36

37 INTRODUCTION

38 Mycotoxins are the most prevalent natural dietary toxins and contaminate up to 70% of
39 global crop production (Eskola *et al.*, 2020). They represent a major issue for food safety
40 (Payros *et al.*, 2021a). These secondary metabolites produced by microscopic fungi are resistant
41 to industrial processes and cooking and contaminate finished processed food. Trichothecenes
42 (TCTs) are one of the most prevalent classes of mycotoxins, comprising over 200 structurally
43 related compounds with a common sesquiterpenoid skeleton (Polak-Śliwińska *et al.*, 2021). The
44 differences in their substitution patterns allow TCTs to be classified into four subgroups. Type
45 A TCTs (TCTs-A) and type B TCTs (TCTs-B) are major food contaminants whereas type C
46 and D TCTs rarely occur in food matrices. Type D TCTs have attracted more attention as indoor
47 pollutants (Gottschalk *et al.*, 2008). TCTs-A include T-2 toxin (T-2), diacetoxyscirpenol
48 (DAS), and the newly discovered form NX (Varga *et al.*, 2015; Pierron *et al.*, 2022). TCTs-B,
49 which are distinguished from TCTs-A by the presence of a ketonic oxygen at C-8, are mainly
50 represented by deoxynivalenol (DON), nivalenol (NIV) or fusarenon-X (FX) (Figure 1). In
51 Europe, almost 50% of cereals are contaminated with DON (Knutsen *et al.*, 2017a), 16% with
52 NIV (Knutsen *et al.*, 2017b), and 10% with FX (Schothorst *et al.*, 2003). T-2 was detected in
53 20% of European cereal samples (Knutsen *et al.*, 2017c) and DAS in 1.5% of European cereals
54 and cereal-based food (Knutsen *et al.*, 2018).

55 The toxicity of DON, the most prevalent foodborne TCT, is well documented. Acute DON
56 poisoning causes vomiting, nausea, and diarrhoea, while chronic exposure results in food
57 refusal, anorexia, reduced body weight gain, and altered immune responses (Terciolo *et al.*,
58 2018; Pinton and Oswald, 2014; Payros *et al.* 2016). At the cellular level, DON triggers
59 ribotoxicity signalled by protein translation arrest and recruitment of MAP kinases, resulting in
60 inflammation, cytotoxicity and apoptosis, depending on the dose and duration of exposure
61 (Payros *et al.*, 2016; Alassane-Kpembi *et al.*, 2013; Payros *et al.*, 2021b). By contrast, other
62 TCTs are largely overlooked in toxicology studies (Seeboth *et al.*, 2010; Alassane-Kpembi *et*
63 *al.*, 2017a; Alassane-Kpembi *et al.*, 2017b; Pierron *et al.*, 2022). Additional studies are needed,
64 both because these TCTs are widely distributed in food, and because they induce not only
65 effects similar to DON, such as ribotoxicity, cytotoxicity, inflammation, vomiting and food
66 refusal, but also specific effects. For example, T-2 induces a potent oral irritation effect with
67 skin blistering (Wyatt *et al.*, 1973), FX exhibits potent antiviral properties (Tani *et al.*, 1995),
68 DAS induces intestinal cell hyperplasia (Weaver, 1981), NIV triggers murine dendritic cells

69 necrosis not documented for other TCTs (Luongo *et al.*, 2010) and NX specifically targets the
70 mitochondria (Soler *et al.*, 2022). The differences between TCTs are also at the molecular level,
71 with differences in the translation step inhibited. Although all TCTs are thought to inhibit
72 peptide elongation (Foroud *et al.*, 2019), T-2, DAS, NIV, and FX also inhibit the initiation step,
73 and DON and FX also inhibit translation termination (Cundliffe *et al.*, 1977).

74 DON, which is not genotoxic on its own, has recently been described as capable of
75 increasing the genotoxicity induced by model or bacterial genotoxins (Payros *et al.*, 2017,
76 Garofalo *et al.*, 2022). This effect is observed with genotoxins with different modes of action,
77 and a role for ribotoxicity has been proposed (Garofalo *et al.*, 2022). In this work, we show that
78 the genotoxicity exacerbation is not only an effect of DON, but also of T-2, DAS, NIV, FX,
79 and NX. Importantly, TCTs do not only exacerbate the genotoxicity induced by a model
80 genotoxin, but also the genotoxicity induced by captan, a pesticide contaminating the food, and
81 the genotoxicity induced by colibactin, a genotoxin produced by *Escherichia coli* bacteria in
82 the gut. Thus, although TCTs are not genotoxic, they could enhance the carcinogenic potential
83 of genotoxins present in the diet or in our microbiota.

84

85 **METHODS**

86 **Toxins and reagents.** DON, NIV, T-2, FX, and DAS were purchased from Sigma-Aldrich
87 (Saint-Quentin Fallavier, France) and Captan by Dr. Ehrenstorfer (GmbH, Germany/CIL-
88 Cluzeau). Phleomycin (PHM) (13.78 mM) was purchased from Invivogen (Toulouse, France).
89 NX, obtained following the methods described by Aitken *et al.*, was a generous gift from D. J.
90 Miller (Aitken *et al.*, 2019). Stock solutions were stored at -20°C. DON (5 mM), NIV (30 mM),
91 T-2 (5 mM), FX (10 mM), DAS (3mM), and captan (50 mM) were dissolved in DMSO; NX
92 (5mM) was dissolved in water.

93

94 **Cell treatments.** Non-transformed rat intestinal epithelial cells (IEC-6, ATCC CRL-1592)
95 were cultured in complete DMEM medium supplemented with 10% foetal calf serum, 1% non-
96 essential amino acids (Fisher scientific, Hampton, USA), and 0.1 U/mL bovine insulin (Sigma-
97 Aldrich), at 37°C with 5% CO₂. The cells were split regularly to maintain exponential growth.
98 A fresh culture was started from a liquid nitrogen stock every 30 passages. The cells were
99 confirmed free of mycoplasma contamination by 16S PCR. For viability assay, cells were
100 seeded in white 96 well plates (Dutscher, Bruxelles, Belgium) and grown to reach ~80%
101 confluence. Cells were then treated for 24 h with various doses of TCTs (or DMSO vehicle)
102 before viability was measured. For ribotoxicity and genotoxicity measurement, cells were

103 seeded in black 96 well plates (Greiner bio-one, Les Ulis, France) and grown to reach ~80%
104 confluence. For ribotoxicity measurement, cells were incubated for 4 h with various doses of
105 TCTs or DMSO vehicle followed by a 30 min incubation with puromycin (Sigma-Aldrich) at
106 a final concentration of 10 $\mu\text{g}/\text{mL}$. For PHM and captan-induced genotoxicity measurement,
107 cells were co-treated for 4 h with 5 μM PHM or 10 μM of captan and various doses of TCTs.

108 **Preparation of colibactin-producing bacteria.** The intestinal carcinogenic *Escherichia coli*
109 strain NC101 that produces the genotoxin colibactin, and the isogenic mutant strain
110 NC101 ΔclbP which do not produce the toxin (Yang *et al.*, 2020) were cultured in Lysogeny-
111 broth (LB) Lennox medium overnight at 37°C with shaking. Epithelial cell-bacteria interaction
112 medium DMEM 25 mM HEPES (Fisher scientific) was inoculated from overnight bacterial
113 cultures and incubated at 37°C with shaking until the bacteria reached an optical density at 600
114 nm of 0.5 before infection.

115

116 **Colibactin-induced genotoxicity measurement.** IEC-6 cells were infected with *E. coli*
117 producing colibactin as described previously (Payros *et al.*, 2017). Briefly, cells were incubated
118 with different doses of TCTs and infected for 4 h with wild type (WT) *E. coli* NC101 or the
119 *clbP* isogenic mutant. Cells were then washed and incubated in complete DMEM medium
120 supplemented with 200 $\mu\text{g}/\text{mL}$ gentamicin and maintained 4 h post-infection in the presence of
121 TCTs or DMSO vehicle, and then fixed for DNA damage measurement.

122

123 **Viability assay.** Cell viability was assayed with the CellTiter-Glo Luminescent Cell Viability
124 Assay (Promega, Charbonnières-les-Bains, France) as described (Khoshal *et al.*, 2019).
125 Luminescence was measured with a spectrophotometer (TECAN Spark, Mannedorf,
126 Switzerland).

127

128 **Ribotoxicity analysis by In-Cell-Western.** Ribotoxicity was measured using protein synthesis
129 inhibition as a surrogate. The measurement of protein synthesis by puromycin labelling was
130 performed as described (Henrich, 2016). Briefly, puromycin was immuno-detected by In-Cell-
131 Western using an anti-puromycin antibody (clone 12D10 diluted 1:5000; Millipore, Molsheim,
132 France). GAPDH, which is constitutively expressed and has a half-life of 8 h (Dani *et al.*, 1984),
133 was used as a control. The anti GAPDH antibody was diluted 1:5000 (ABS16; Millipore).
134 Secondary antibodies were diluted 1:5000 (IRDye 800CW; Rockland, and IRDye 680RD
135 Licor). Puromycin signal was normalized with the average fluorescence of puromycin-labelled
136 control cells (Henrich, 2016).

137

138 **Quantification of DNA damage by In-Cell-Western.** In-Cell-Western was performed as
139 previously described (Martin *et al.*, 2013; Tronnet and Oswald, 2018; Theumer *et al.*, 2018).
140 Briefly, fixed cells were permeabilized and stained with the primary antibody anti- γ H2AX
141 (20E3 diluted 1:200; Cell Signalling, Saint-Quentin en Yvelines, France). Secondary antibody
142 (IRDye 800CW diluted 1:1000; Rockland) and RedDot2 DNA marker (Biotium) were
143 measured at 680 and 800 nm with a Sapphire Biomolecular Imager (Azure Biosystems). The
144 genotoxic index was calculated by dividing the γ H2AX signal by the corresponding DNA
145 fluorescence and normalized with the average signal in control cells (Tronnet and Oswald,
146 2018).

147

148 **Data analysis.** GraphPad Prism 8.0 was used to calculate concentrations that inhibited the cell
149 viability by 20% (IC₂₀), and the protein synthesis by 20% (20% PSI level), performing a four-
150 parameter nonlinear regression model (sigmoidal dose-response analysis). Profile-likelihood
151 confidence intervals were calculated from the nonlinear regressions. One-way analysis of
152 variance (ANOVA) followed by Bonferroni's multiple comparison were performed. The data are
153 expressed as mean \pm SEM.

154

155 **RESULTS**

156 **Trichothecenes induce a dose-dependent reduction in cell viability.** As the intestinal tract is
157 the primary target of TCTs, the non-transformed intestinal epithelial cell line IEC-6 was used.
158 Cytotoxicity was first evaluated 4 h and 8 h after TCTs treatment, and no cytotoxicity was
159 detected (Table S1). The effect of TCTs on cell viability was then evaluated 24 h after treatment,
160 and we observed a dose-dependent inhibition of viability induced by DON, NIV, T-2, FX, DAS
161 and NX (Figure 2A). IC₂₀ values, which correspond to the dose inducing a 20% reduction of
162 cell viability, were calculated for each TCT (Figure 2B). For cytotoxicity, TCTs were classified
163 as follows: T-2>DAS>FX>NIV>NX>DON.

164

165 **Trichothecenes induce a dose-dependent ribotoxicity.** Ribotoxicity is the main mode of
166 action of TCTs (Pestka, 2010). To quantify the ribotoxicity of the TCTs, we examined
167 translational inhibition, assessed by the incorporation of the protein translation marker
168 puromycin in newly synthesized peptides (Henrich, 2016). The incorporated puromycin was
169 quantified by immunofluorescence. All the TCTs induced a dose-dependent ribotoxicity
170 (Figure 3A). Treatment with TCTs did not induce a drop in GAPDH levels (which has an 8 h

171 half-life), confirming that puromycin specifically labelled newly synthesized peptides (Figure
172 3A, Figure S2). The doses inducing a 20% reduction in protein synthesis were calculated
173 (Figure 3B). For their ribotoxic effect, TCTs were classified as follows: T-
174 2>DAS>FX>NIV>NX≥DON.

175

176 **Trichothecenes exacerbate DNA damage induced by the drug phleomycin.** The genotoxic
177 exacerbation properties of TCTs were first evaluated with phleomycin (PHM), a genotoxin
178 commonly used as a model for genotoxicity assessments (Chen and Stubbe, 2005). IEC-6 cells
179 were treated for 4 h with PHM and/or TCTs. As expected, cells treated with PHM alone
180 exhibited DNA damage signalled by the γ H2AX marker (Rogakou *et al.*, 1998). TCTs alone
181 did not induce γ H2AX, indicating that they are not genotoxic by themselves. In contrast, all the
182 TCTs induced exacerbation of PHM-induced DNA damage, in a dose-dependent manner
183 (Figure 4A). A significant increase occurred from 1 μ M for DON, 3 μ M for NX, 10 nM for T-
184 2, 0.3 μ M for FX, 30 nM for DAS, and 3 μ M for NX (Figure 4B). The exacerbation of
185 genotoxicity did not induce cell detachment, indicating that this effect was not a consequence
186 of massive cell death (Figure 4, Table S1).

187

188 **Trichothecenes exacerbate DNA damage induced by captan, a pesticide which**
189 **contaminates food.** We then tested the ability of TCTs to exacerbate genotoxicity induced by
190 a food-contaminating genotoxin, such as the pesticide captan, which can be found in fruits,
191 vegetables, and cereals (Shinde *et al.*, 2019). For this purpose, IEC-6 cells were exposed to
192 captan and/or TCTs for 4 h. Captan alone induced DNA damage, and TCTs induced an
193 exacerbation of the genotoxicity of captan, in a dose-dependent manner. Significant increase
194 occurred from 3 μ M for DON and NX, 1 nM for T-2, 1 μ M for FX, and 3 nM for DAS, and did
195 not induce cell death (Figure 5, Table S1).

196

197 **Trichothecenes exacerbate genotoxicity induced by colibactin, a genotoxin produced by**
198 **members of the intestinal microbiota.** We then determined whether TCTs also exacerbate
199 genotoxicity induced by a bacterial genotoxin produced by the intestinal microbiota, colibactin.
200 The genotoxicity of colibactin was measured by infecting IEC-6 cells with the live colibactin-
201 producing bacterium *Escherichia coli* NC101. Since colibactin is unstable and is not purifiable,
202 direct contact between live colibactin-producing *E. coli* strain and eukaryotic cells is required
203 to induce DNA damage (Chagneau *et al.*, 2022; Nougayrède *et al.*, 2006; Bossuet-Greif *et al.*,
204 2018). Cells were infected with strain NC101 and either co-treated with TCTs or not. Cells

205 infected with the WT strain showed an increase in their γ H2AX signal, resulting from colibactin
206 damage, whereas cells infected with the NC101 Δ *clbP* strain, which is impaired for colibactin
207 synthesis, did not show DNA damage (Figures 6, S1). By contrast, TCTs-treated and WT-
208 infected cells exhibited exacerbation of colibactin-induced DNA damage, which increased with
209 TCT dosage. A significant increase occurred at 3 μ M for DON, NX and NIV, 1 nM for T-2, 0.3
210 μ M for FX, and 10 nM for DAS (Figure 6), and was not associated with cell death (Table S1).
211 Exacerbation of DNA damage was not associated with increased colibactin production by TCT-
212 treated bacteria, nor was it associated with an impact of TCTs on bacterial growth
213 (Supplementary methods 1, Figure S1).

214

215 DISCUSSION

216 Food contamination by TCTs is a public health issue of the utmost importance. TCTs
217 levels in foods are indeed high and may even increase in the future, in part due to climate change
218 (Van Der Fels, 2016). DON, which is not genotoxic, was recently described as a genotoxicity
219 enhancer (Garofalo *et al.*, 2022; Payros *et al.*, 2017). In this work, we show that this is not only
220 an effect of DON, but also a novel effect attributable to at least five other TCTs: NIV, T-2, FX,
221 DAS and the recently discovered NX toxin. These TCTs exacerbate not only the genotoxicity
222 induced by the model genotoxin phleomycin, but also the genotoxicity induced by captan, a
223 pesticide with genotoxic properties, and by colibactin, a bacterial genotoxin produced in the
224 gut. For this newly identified effect, TCTs were classified as follows: T-
225 2>DAS>FX>NIV \geq DON \geq NX.

226 The cytotoxicity of TCTs was compared in non-transformed IEC-6 intestinal cells. Our
227 data show that TCTs, which were not cytotoxic after a treatment lasting 4 h or 8 h, induced a
228 dose-dependent inhibition of cell viability after 24 h. These data allowed the classification of
229 TCTs as follows: T-2>DAS>FX>NIV>NX>DON. Although, to the best of our knowledge, this
230 is the first direct comparison and ranking of TCTs' cytotoxicity in IEC-6 cells, the classification
231 is consistent with the literature. T-2 toxin is indeed known as the most toxic TCT, with IC₂₀
232 about 1000 times greater than others (Fernández-Blanco, 2018). DAS is slightly less cytotoxic
233 than T-2, but more than FX (Moon, 2003), and FX is more cytotoxic than NIV and DON
234 (Aupanun *et al.*, 2019; Alassane-Kpembé *et al.*, 2017a). We observed that IEC-6 cells exhibit a
235 modest sensitivity to DON. As a matter of fact, after 24 h of treatment, we found an IC₂₀ of
236 20.2 μ M when others found IC₂₀ of \approx 0.5 μ M in IPEC-1 cells, or \approx 3 μ M in Caco-2 cells
237 (Alassane-Kpembé *et al.*, 2015; Pierron *et al.*, 2022). Our results are consistent with those
238 obtained by Bianco *et al.*, who found an IC₅₀ for DON of 50.2 μ M in IEC-6 cells, confirming

239 the limited sensitivity of this cell line (Bianco *et al.*, 2012). In addition, our results highlight
240 that NX is approximately twice as cytotoxic as DON in IEC-6 cells. This result is consistent
241 with the results of Pierron *et al.* which showed a higher inflammatory potential for NX
242 compared to DON in porcine intestinal explants (Pierron *et al.*, 2022). In contrast, the literature
243 shows that NX-induced cytotoxicity is comparable to that of DON in HT-29 and Caco-2 cells
244 (Varga *et al.*, 2018; Pierron *et al.*, 2022). Importantly, the doses of TCTs that were cytotoxic
245 after 24 h of exposure were higher than the doses that exacerbated genotoxicity (Table 1). This
246 indicates that non-cytotoxic doses of TCTs exacerbate genotoxicity. Because DNA damage is
247 a source of genetic mutations through repair errors, this result raises questions about the fate of
248 these cells (Basu, 2018). Cells co-exposed to genotoxins and TCTs survive and could therefore
249 pursue their cell cycle and division following repair of DNA damage. Further studies are needed
250 to examine whether cells co-exposed to TCTs and genotoxins could accumulate mutations,
251 ultimately resulting in cellular transformation.

252 In this work, we also classified TCTs for their ribotoxicity. The ranking T-
253 2>DAS>FX>NIV>NX≥DON parallels that obtained for cytotoxicity and is coherent with the
254 structures of TCTs. The most ribotoxic TCTs carry substitutions thought to improve binding to
255 the ribosome, such as the isovaleryl group at C₈ in T-2 or the acetyl groups at C₄ and C₁₅ in
256 DAS (Wu *et al.*, 2013; Wang *et al.*, 2021). Differences in TCTs' ribotoxicity may also be related
257 to divergences in structural rearrangements induced by ribosome binding (Garreau de
258 Loubresse *et al.*, 2014). Depending on the structure of TCTs, structural rearrangements could
259 differ and induce variations in the mode of protein synthesis inhibition. We have previously
260 suggested that DON-induced ribotoxicity is involved in the genotoxicity exacerbation
261 phenotype. Indeed, ribotoxic compounds reproduced the effect, while the non-ribotoxic DON
262 derivative DOM-1, did not (Garofalo *et al.*, 2022). The correlation between TCTs' ribotoxic
263 and genotoxicity exacerbating doses observed in this work (Table 1) support this hypothesis.
264 Interestingly, TCTs with substitutions that increase affinity to the ribosome have a greater
265 capacity to exacerbate genotoxicity. This suggests that there is a structure-function link between
266 ribotoxicity and genotoxicity exacerbation. TCTs could be classified into 3 subgroups
267 according to their capacity to exacerbate the genotoxicity, with regard to their affinity with the
268 ribosome: T-2, DAS > FX > NIV, NX, DON.

269 Several mechanism could be involved the ribosome-dependent exacerbation of
270 genotoxicity. In response to DNA damage, cells reprogram their gene expression to synthesize
271 proteins of the DNA damage response (Spriggs, Bushell and Willis, 2010). TCTs-induced
272 ribotoxicity could disrupt the production of these stress response proteins. Through their

273 ribotoxic effect, TCTs can induce inflammation (Pestka, 2010; Garcia et al 2018), which
274 represses the DNA damage response (Jaiswal *et al.*, 2000). Finally, it has been documented that
275 DON activates the protein kinase R (PKR), which triggers inhibition of the DNA damage repair
276 and sensitizes cells to DNA damage (Zhou *et al.*, 2014). As they share structural similarities
277 with DON, TCTs could also recruit PKR and induce sensitization to DNA damage. Further
278 work is required to understand how ribotoxicity results in this novel effect of TCTs.

279 We observed that exacerbation of genotoxicity occurred at realistic doses of TCTs. The
280 European Food Safety Authority (EFSA) established a no observable adverse effect level
281 (NOAEL) for DON of 100 µg/kg body weight (bw)/day (Knutsen *et al.* 2017a), and 65 µg/kg
282 bw/day for DAS (Knutsen *et al.*, 2018). The Benchmark Dose Limit (BMDL₁₀) for NIV is 350
283 µg/kg bw/day (Knutsen *et al.*, 2017b), and 3.3 µg/kg bw/day for T-2 (Knutsen *et al.*, 2017c).
284 Estimating, as Maresca *et al.*, 2013, that for a human weighing 70 kg, the small intestine content
285 is 1L, these doses can be converted to intestinal concentrations of 23.6 µM DON, 0.5 µM T-2,
286 12.5 µM DAS, and 78.4 µM NIV. Our study shows no effect doses for genotoxicity
287 exacerbation well below these reference values, with 1 µM, 3 nM, 10 nM, and 3 µM for DON,
288 T-2, DAS and NIV, respectively. We observed that structurally related TCTs displayed
289 comparable effects, and could therefore be classified into 3 subgroups: T-2, DAS > FX > NIV,
290 NX, DON. As TCTs frequently co-occur in foodstuffs (Alassane-Kpembé *et al.*, 2017b), it
291 would be appropriate to set group TDIs for TCTs, as it has been done for other groups of
292 structurally related mycotoxins (Steinkellner *et al.* 2019).

293 The exacerbation effect occurred with captan, a pesticide which induces *in vitro* DNA
294 damage (Fernandez-Vidal *et al.*, 2019). Captan can contaminate fruits and vegetables, but also
295 cereals, which are the main source of TCTs (Shinde *et al.*, 2019). Captan has been associated
296 with multiple myeloma in farmers (Presutti *et al.*, 2016), and is classified by the European
297 Commission as “suspected of causing cancer” (European Commission, 2008). Notably, the
298 exacerbation effect occurred at realistic doses of captan. The NOAEL for captan is indeed 25
299 mg/kg bw per day (Anastassiadou *et al.*, 2020), which corresponds to an intestinal concentration
300 of 5.8 mM. Here, the exacerbated genotoxic effect of captan was observed with a dose as low
301 as 10 µM, well below the NOAEL. Interestingly, TCTs also exacerbate the effect of colibactin,
302 an endogenous genotoxin produced by the intestinal microbiota throughout the host’s life.
303 Indeed, approximately 15% of 3-day-old neonates are colonized by colibactin-producing *E. coli*
304 (Payros *et al.*, 2014), and 25% of adults harbour these bacteria (Putze *et al.*, 2009; Tenaillon *et*
305 *al.*, 2010; Johnson *et al.*, 2008). In addition, the prevalence of the B2 phylogenetic group of *E.*
306 *coli*, which includes up to 50% of colibactin-producing strains, is increasing in developed

307 countries (Tenailon *et al.*, 2010). The intestinal microbiome also encodes other bacterial
308 genotoxins such as cytolethal distending toxins (Taieb *et al.*, 2016). Thus, humans are
309 potentially co-exposed to TCTs together with endogenous genotoxins produced by the
310 microbiota as well as multiple exogenous diet-borne genotoxins, such as captan, and other
311 genotoxic pesticides such as glyphosate (International Agency for Research on Cancer, 2017),
312 alcohol-derivatives (Brooks *et al.*, 2014), and components of red meat (Bastide *et al.*, 2011).
313 Given the high prevalence of TCTs in foods, it is conceivable that TCTs could exacerbate the
314 effect of the multiple genotoxic agents to which we are exposed.

315

316 **CONCLUSION**

317 We report that even though TCTs are not genotoxic by themselves, these contaminants promote
318 the genotoxicity of genotoxins which are in the diet, such as pesticides, or are produced by the
319 intestinal microbiota. Considering the wide prevalence of both TCTs and genotoxins, a large
320 part of the population could be impacted by this novel effect. This is alarming because DNA
321 damage drives cancer development (Basu, 2018). A preliminary report on a large-scale
322 epidemiological study in the European Union has suggested a link between long-term exposure
323 to DON and an increased risk of colon cancer (Huybrechts *et al.*, 2019). If confirmed,
324 exacerbation of DNA damage by DON could be a key to explaining this epidemiological link.
325 Here, we show that DON is not the only dietary TCT to exhibit this genotoxicity-exacerbating
326 property. There is an urgent need for additional studies on the impact of TCTs on carcinogenesis
327 induced by other environmental toxicants.

328

329 **ACKNOWLEDGMENTS**

330 We thank David J. Miller for the gift of NX. We thank Julien Vignard (Toxalim) for the
331 scientific input. We are grateful to Elisha Oliver for editing the language. This work was
332 supported by grants from the French Agence Nationale de la Recherche (Genofood ANR-19-
333 CE34 and GenoMyc ANR-22-CE34). MG was supported by a fellowship from the French
334 ministry for Higher Education and Research.

335

336 **REFERENCES**

337 Aitken A., Miller J.D. and McMullin D.R. 2019. 'Isolation, chemical characterization,
338 and hydrolysis of the trichothecene 7 α -hydroxy, 15-deacetylcalonecitrin (3ANX) from
339 *Fusarium graminearum* DAOMC 242077', *Tetrahedron Lett.*, 60:852–856.
340 doi:10.1016/j.tetlet.2019.02.025.

341 Alassane-Kpembé I., Kolf-Clauw M., Gauthier T., Abrami R., Abiola F.A., Oswald I.P.,
342 Puel, O. 2013. 'New insights into mycotoxin mixtures: The toxicity of low doses of Type B
343 trichothecenes on intestinal epithelial cells is synergistic', *Toxicol. Appl. Pharmacol.*, 272:191–
344 198. doi:10.1016/j.taap.2013.05.023.

345 Alassane-Kpembé I., Puel O., Oswald I.P. 2015. 'Toxicological interactions between the
346 mycotoxins deoxynivalenol, nivalenol and their acetylated derivatives in intestinal epithelial
347 cells', *Arch Toxicol.*, 8:1337:1346. doi: 10.1007/s00204-014-1309-4.

348 Alassane-Kpembé I., Gerez J.R., Cossalter A.M., Neves M., Laffitte J., Naylies C., Lippi
349 Y., Kolf-Clauw M., Bracarense AP.F.L., Pinton P., Oswald I.P. 2017a. 'Intestinal toxicity of
350 the type B trichothecene mycotoxin fusarenon-X: whole transcriptome profiling reveals new
351 signaling pathways', *Sci. Rep.* 7:7530. doi: 10.1038/s41598-017-07155-2.

352 Alassane-Kpembé I., Puel O., Pinton P., Cossalter A.M., Chou T.C., Oswald I.P. 2017b.
353 'Co-exposure to low doses of the food contaminants Deoxynivalenol and Nivalenol has a
354 synergistic inflammatory effect on intestinal explants', *Arch Toxicol.* 91: 2677-87. doi:
355 10.1007/s00204-016-1902-9.

356 Anastassiadou M., Arena M., Auteri D., Brancato A., Bura L., Carrasco Cabrera L.,
357 Chaideftou E., Chiusolo A., Crivellente F., De Lentdecker C. *et al.* 2020. 'Peer review of the
358 pesticide risk assessment of the active substance captan', *EFSA Journal*, 18:6230.
359 doi :10.2903/j.efsa.2020.6230.

360 Aupanun S., Poapolathep S., Phuektes P., Giorgi M., Zhang Z., Oswald I.P, Poapolathep
361 A. 2019. 'Individual and combined mycotoxins deoxynivalenol, nivalenol, and fusarenon-X
362 induced apoptosis in lymphoid tissues of mice after oral exposure', *Toxicon.*, 165:83-94. doi:
363 10.1016/j.toxicon.2019.04.017.

364 Bastide N.M., Pierre F.H., Corpet D.E. 2011. 'Heme iron from meat and risk of
365 colorectal cancer: a meta-analysis and a review of the mechanisms involved', *Cancer Prev.*
366 *Res. (Phila)*, 4:177-84. doi: 10.1158/1940-6207.CAPR-10-0113.

367 Basu A.K. 2018. 'DNA Damage, Mutagenesis and Cancer', *Int. J. Mol. Sci.*, 19:970.
368 doi: 10.3390/ijms19040970.

369 Bianco G., Fontanella B., Severino L., Quaroni A., Autore G., Marzocco S. 2012.
370 'Nivalenol and deoxynivalenol affect rat intestinal epithelial cells: a concentration related
371 study', *PLoS One*, 7:e52051. doi:10.1371/journal.pone.0052051.

372 Bossuet-Greif N., Vignard J., Taieb F., Mirey G., Dubois D., Petit C., Oswald E.,
373 Nougayrède J.P. 2018. 'The Colibactin Genotoxin Generates DNA Interstrand Cross-Links in
374 Infected Cells', *mBio*, 9: e02393. doi:10.1128/mBio.02393-17.

375 Brooks P.J., Zakhari S. 2014. 'Acetaldehyde and the genome: beyond nuclear DNA
376 adducts and carcinogenesis', *Environ. Mol. Mutagen.*, 55:77-91. doi: 10.1002/em.21824.

377 Chagneau C.V., Payros D., Tang-Fichaux M., Auvray F., Nougayrède J.P., Oswald E.
378 2022. 'The pks island: a bacterial Swiss army knife?', *Trends Microbiol.* doi:
379 10.1016/j.tim.2022.05.01.

380 Chen J., Stubbe J. 2005. 'Bleomycins: towards better therapeutics', *Nat. Rev. Cancer*,
381 5:102–112. doi:10.1038/nrc1547.

382 Cundliffe E., Davies J.E. 1977. 'Inhibition of initiation, elongation, and termination of
383 eukaryotic protein synthesis by trichothecene fungal toxins', *Antimicrob Agents Chemother.*,
384 11:491-9. doi: 10.1128/AAC.11.3.491.

385 Dani C., Piechaczyk M., Audigier Y., El Sabouty S., Cathala G., Marty L., Fort P.,
386 Blanchard J.M., Jeanteur P. 1984. 'Characterization of the transcription products of
387 glyceraldehyde 3-phosphate-dehydrogenase gene in HeLa cells', *Eur J Biochem.* 14:299-304.
388 doi: 10.1111/j.1432-1033.1984.tb08552.x.

389 Eskola, M., Elliott, C.T., Hajšlov, J., Steiner, D., Krska, R. 2020. 'Towards a dietary-
390 exposome assessment of chemicals in food: an update on the chronic health risks for the
391 European consumer', *Crit. Rev. Food Sci. Nutr.*, 60:1890–1911. doi:10.1080/10408398.
392 2019.1612320.

393 European Commission. 2008. 'Regulation No 1272/2008 of the European Parliament
394 and of the Council of 16 December 2008 on classification, labelling and packaging of
395 substances and mixtures, amending and repealing Directives 67/548/EEC and 1999 /45/EC and
396 amending Regulation (EC) No 1907/2006'. *Official journal of the European Union*, 354:1-
397 1355.

398 Fernández-Blanco C., Elmo L., Waldner T., Ruiz M.J. 2018. 'Cytotoxic effects induced
399 by patulin, deoxynivalenol and toxin T2 individually and in combination in hepatic cells
400 (HepG2)', *Food Chem Toxicol.*, 120:12-23. doi: 10.1016/j.fct.2018.06.019.

401 Fernandez-Vidal A., Arnaud L.C., Maumus M., Chevalier M., Mirey G., Salles B.,
402 Vignard J., Boutet-Robinet E. 2019. 'Exposure to the Fungicide Captan Induces DNA Base
403 Alterations and Replicative Stress in Mammalian Cells', *Environ. Mol. Mutagen.* 3:286-297.
404 doi: 10.1002/em.22268.

405 Foroud N.A., Baines D., Gagkaeva T.Y., Thakor N., Badea A., Steiner B., Bürstmayr
406 M., Bürstmayr H. 2019. 'Trichothecenes in Cereal Grains – An Update', *Toxins*, 11:634. doi:
407 10.3390/toxins11110634.

408 Garcia G.R., Payros D., Pinton P., Dogi C.A., Laffitte J., Neves M., Gonzalez-Pereyra
409 M.L., Cavaglieri L.R., Oswald I.P. 2018. Intestinal toxicity of deoxynivalenol is limited by
410 *Lactobacillus rhamnosus* RC007 in pig jejunum explants. *Arch Toxicol.* 92: 983-993. doi:
411 10.1007/s00204-017-2083-x

412
413

414 Garreau de Loubresse N., Prokhorova I., Holtkamp W., Rodnina V., Yusupova G.,
415 Yusupov M., 2014. 'Structural basis for the inhibition of the eukaryotic ribosome', *Nature*, 513:
416 517–522. doi:10.1038/nature13737.

417 Garofalo M., Payros, D., Oswald E., Nougayrède J.P., Oswald I.P. 2022. 'The foodborne
418 contaminant deoxynivalenol exacerbates DNA damage caused by a broad spectrum of
419 genotoxic agents', *STOTEN*, 820:153280. doi:10.1016/j.scitotenv.2022.153280.

420 Gottschalk C., Bauer J., Meyer K. 2008. 'Detection of satratoxin g and h in indoor air
421 from a water-damaged building', *Mycopathol.*, 166:103-7. doi: 10.1007/s11046-008-9126-z.

422 Henrich C.J. 2016. 'A Microplate-Based Nonradioactive Protein Synthesis Assay:
423 Application to TRAIL Sensitization by Protein Synthesis Inhibitors', *PloS One*, 11: e0165192.
424 doi:10.1371/journal.pone.0165192.

425 Huybrechts K., Claeys L., Ferrari P., Altieri A., Arcella D., Papadimitriou C.,
426 Casagrande C., Nicolas G., Biessy C., Zavadil J., Gunter M., De Saeger S., De Boevre M. 2019.
427 'Impact of chronic multi-mycotoxin dietary exposure on colorectal and liver cancer risk in
428 Europe', *World Mycotoxin Forum - Book of Abstracts*, p. 70.

429 International Agency for Research on Cancer (IARC) Working Group on the Evaluation
430 of Carcinogenic Risks to Humans. 2017. 'Some Organophosphate Insecticides and Herbicides',
431 Lyon (FR), vol. 112. Bookshelf ID: NBK436774.

432 Jaiswal M., Lauroso, N.F., Burgart L.J. 2000. 'Inflammatory Cytokines Induce DNA
433 damage and Inhibit DNA repair in Cholangiocarcinoma Cells by a Nitric Oxide-dependent
434 Mechanism', *Cancer Res.*, 60:184-190.

435 Johnson J.R., Johnston B., Kuskowski M.A., Nougayrede, J.P., Oswald E. 2008.
436 'Molecular epidemiology and phylogenetic distribution of the Escherichia coli pks genomic
437 island', *J. Clin. Microbiol.* 46: 3906–3911. doi: 10.1128/JCM.00949-08

438 Khoshal A.K., Novak B., Martin P.G.P., Jenkins T., Neves M., Schatzmayr G., Oswald
439 I.P., Pinton P. 2019. 'Co-occurrence of DON and Emerging Mycotoxins in Worldwide Finished
440 Pig Feed and Their Combined Toxicity in Intestinal Cells', *Toxins (Basel)*, 12:727. doi:
441 10.3390/toxins11120727.

442 Knutsen H.K., Alexander, J., Barregard, L., Bignami, M., Bruschiweiler, B., Ceccatelli,
443 S., Cottrill, B., Dinovi, M., Grasl-Kraupp, B., Hogstrand, C. *et al.* 2017a. ‘Risks to human and
444 animal health related to the presence of deoxynivalenol and its acetylated and modified forms
445 in food and feed’, *EFSA Journal*, 15: e04718. doi: 10.2903/j.efsa.2017.4718.

446 Knutsen H.K., Barregard L., Bignami M., Bruschiweiler B., Ceccatelli S., Cottrill B.,
447 Dinovi M., Edler L., Grasl-Kraupp B., Hogstrand C. *et al.* 2017b. ‘Appropriateness to set a
448 group health based guidance value for nivalenol and its modified forms’, *EFSA Journal*,
449 15:4751. doi: 10.2903/j.efsa.2017.4751.

450 Knutsen H.K., Barregard L., Bignami M., Bruschiweiler B., Ceccatelli S., Cottrill B.,
451 Dinovi M., Edler L., Grasl-Kraupp B., Hoogenboom L. *et al.* 2017c. ‘Appropriateness to set a
452 group health based guidance value for T2 and HT2 toxin and its modified forms’, *EFSA*
453 *Journal*, 15: 4655. doi: 10.2903/j.efsa.2017.4655.

454 Knutsen H.K., Alexander J., Barregard L., Bignami M., Bruschiweiler B., Ceccatelli S.,
455 Cottrill B., Dinovi M., Grasl-Kraupp B., Hogstrand C. *et al.* 2018. Risk to human and animal
456 health related to the presence of 4,15- diacetoxyscirpenol in food and feed’, *EFSA Journal*,
457 16:8. doi:10.2903/j.efsa.2018.5367.

458 Luongo D., Severino L., Bergamo P., D’Arienzo R., Rossi M. 2010. ‘Trichothecenes
459 NIV and DON modulate the maturation of murine dendritic cells’, *Toxicol.*, 55:73-80. doi:
460 10.1016/j.toxicol.2009.06.039.

461 Maresca M. 2013. ‘From the gut to the brain: journey and pathophysiological effects of
462 the food-associated trichothecene mycotoxin deoxynivalenol’, *Toxins (Basel)*, 23:784-820. doi:
463 10.3390/toxins5040784.

464 Martin P., Marcq I., Magistro G., Penary M., Garcia C. Payros D., Boury M., Olier M.,
465 Nougayrède J.P., Audebert M., Chalut C., Schubert S., Oswald, E. 2013. ‘Interplay between
466 Siderophores and Colibactin Genotoxin Biosynthetic Pathways in *Escherichia coli*’, *PLoS*
467 *Pathog.*, 9:e1003437. doi:10.1371/journal.ppat.1003437.

468 Moon Y., Uzarski R., Pestka J.J. 2003. ‘Relationship of trichothecene structure to COX-
469 2 induction in the macrophage: selective action of type B (8-keto) trichothecenes’, *J. Toxicol.*,
470 *Environ Health A.* 66:1967-83. doi: 10.1080/713853950.

471 Nougayrède J.P., Homburg S., Taieb F., Boury M., Brzuszkiewicz E., Gottschalk G.,
472 Buchrieser C., Hacker J., Dobrindt U., Oswald E. 2006. ‘*Escherichia coli* Induces DNA
473 Double-Strand Breaks in Eukaryotic Cells’, *Science*, 313: 848–851.
474 doi:10.1126/science.1127059.

475 Payros D., Secher T., Boury M., Brehin C., Ménard S., Salvador-Cartier C., Cuevas-
476 Ramos G., Watrin C., Marcq I., Nougayrède J.P., *et al.* 2014. ‘Maternally acquired genotoxic
477 *Escherichia coli* alters offspring’s intestinal homeostasis’, *Gut Microbes*, 5: 313–512.
478 doi:10.4161/gmic.28932.

479 Payros D., Alassane-Kpembi I., Pierron A., Loiseau N., Pinton P., Oswald I.P. 2016.
480 ‘Toxicology of deoxynivalenol and its acetylated and modified forms’, *Arch. Toxicol.*, 90:
481 2931–2957. doi:10.1007/s00204-016-1826-4.

482 Payros D., Dobrindt U., Martin P., Secher T., Bracarense A.P.F.L., Boury M., Laffitte
483 J., Pinton P., Oswald E., Oswald I.P. 2017. ‘The Food Contaminant Deoxynivalenol
484 Exacerbates the Genotoxicity of Gut Microbiota’, *mBio*, 8: e007-17. doi:10.1128/mBio.00007-
485 17.

486 Payros D., Garofalo, M., Pierron A., Soler-Vasco L., Al-Ayoubi C., Maruo, V.M.,
487 Alassane- Kpembi I., Pinton P., Oswald, I.P. 2021a. ‘Mycotoxins in human food: a challenge
488 for research’. *Cah. Nutr. Diet.*, 56: 170–183. doi:10.1016/j.cnd.2021.02.001.

489 Payros D., Alassane-Kpembi I., Laffitte J., Lencina C., Neves M., Bracarense A.P.,
490 Pinton P., Ménard S., Oswald I.P. 2021b. ‘Dietary Exposure to the Food Contaminant
491 Deoxynivalenol Triggers Colonic Breakdown by Activating the Mitochondrial and the Death
492 Receptor Pathways’. *Mol. Nutr. Food. Res.* 65:e2100191. doi: 10.1002/mnfr.202100191.

493 Pestka, J.J. 2010. ‘Deoxynivalenol-Induced Proinflammatory Gene Expression:
494 Mechanisms and Pathological Sequelae’, *Toxins*, 2:1300–1317. doi:10.3390/toxins2061300.

495 Pierron A., Neves M., Puel S., Lippi Y., Soler L., Miller J.D., Oswald I.P. 2022.
496 ‘Intestinal toxicity of the new type A trichothecenes, NX and 3ANX’, *Chemosphere*. 288:
497 132415. doi:10.1016/j.chemosphere.2021.132415.

498 Pinton P. and Oswald I.P. 2014. ‘Effect of Deoxynivalenol and Other Type B
499 Trichothecenes on the Intestine: A Review’, *Toxins*, 6: 1615-1643. doi:
500 10.3390/toxins6051615.

501 Polak-Śliwińska M., Paszczyk B. 2021. ‘Trichothecenes in Food and Feed, Relevance
502 to Human and Animal Health and Methods of Detection: A Systematic Review’, *Molecules*,
503 26:454. doi:10.3390/molecules26020454.

504 Presutti R., Harris S.A., Kachuri L., Spinelli J.J., Pahwa M., Blair A., Zahm S.H., Cantor
505 K.P., Weisenburger D.D, Pahwa P. et al. 2016. ‘Pesticide exposures and the risk of multiple
506 myeloma in men: An analysis of the North American Pooled Project’, *Int. J. Cancer*, 139:1703-
507 1714. doi: 10.1002/ijc.30218.

508 Putze J., Hennequin C., Nougayrède J.P., Zhang W., Homburg S., Karch H., Bringer
509 M.A., Fayolle C., Carniel E., Rabsch W., Oelschlaeger T.A., Oswald E., Forestier C., Hacker
510 J., Dobrindt U. 2009. 'Genetic structure and distribution of the colibactin genomic island among
511 members of the family *Enterobacteriaceae*', *Infect Immun.*, 77:4696-703. doi:
512 10.1128/IAI.00522-09.

513 Rogakou E.P., Pilch D.R., Orr A.H., Ivanova V.S., Bonner W.M. 1998. 'DNA Double-
514 stranded Breaks Induce Histone H2AX Phosphorylation on Serine 139', *J. Biol. Chem.*, 273:
515 5858–5868. doi:10.1074/jbc.273.10.5858.

516 Schothorst R.C. and van Egmond H.P. 2003. 'Report from SCOOP task 3.2.10:
517 collection of occurrence data of *Fusarium* toxins in food and assessment of dietary intake by
518 the population of EU member states. Subtask: trichothecenes', *Toxicol. Lett.*, 153:133-43. doi:
519 10.1016/j.toxlet.2004.04.045.

520 Seeboth J., Solinhac R., Oswald I.P., Guzylack-Piriou L. 2012. 'The fungal T-2 toxin
521 alters the activation of primary macrophages induced by TLR-agonists resulting in a decrease
522 of the inflammatory response in pigs', *Vet Res.* 43:35. doi: 10.1186/1297-9716-43-35.

523 Shinde R., Shiragave P., Lakade A., Thorat P., Banerjee K. 2019. 'Multi-residue
524 analysis of captan, captafol, folpet, and iprodione in cereals using liquid chromatography with
525 tandem mass spectrometry', *Food Addit. Contam. Part A Chem. Anal. Control Expo. Risk*
526 *Assess.*, 36:1688-1695. doi: 10.1080/19440049.2019.1662953.

527 Soler L., Miller I., Terciolo C., Hummel K., Nöbauer K., Neves M., Oswald I.P. 2022.
528 'Exposure of intestinal explants to NX, but not to DON, enriches the secretome in mitochondrial
529 proteins', *Arch. Toxicol.* doi: 10.1007/s00204-022-03318-x.

530 Spriggs K.A., Bushell M. and Willis A.E. 2010. 'Translational Regulation of Gene
531 Expression during Conditions of Cell Stress', *Molecular Cell*, 40: 228–237.
532 doi:10.1016/j.molcel.2010.09.028.

533 Steinkellner H., Binaglia M., Dall'Asta C., Gutleb A.C., Metzler M., Oswald I.P.,
534 Parent-Massin D., Alexander J. 2019. Combined hazard assessment of mycotoxins and their
535 modified forms applying relative potency factors: Zearalenone and T2/HT2 toxin. *Food Chem*
536 *Toxicol.* 131:110599. doi: 10.1016/j.fct.2019.110599.

537 Taieb F., Petit C., Nougayrède J.P., Oswald E. 2016. 'The Enterobacterial Genotoxins:
538 Cytotoxic Distending Toxin and Colibactin', *EcoSal Plus*, 7:1. doi: 10.1128/ecosalplus.ESP-
539 0008-2016. PMID: 27419387.

540 Tani N., Dohi Y., Onji Y., Yonemasu K. 1995. 'Antiviral activity of trichothecene
541 mycotoxins (deoxynivalenol, fusarenon-X, and nivalenol) against herpes simplex virus types 1

542 and 2', *Microbiol Immunol.*, 39: 635-7. doi: 10.1111/j.1348-0421.1995.tb02254.x.

543 Tenailon O., Skurnik D., Picard B., Denamur E. 2010. 'The population genetics of
544 commensal *Escherichia coli*', *Nat. Rev. Microbiol.*, 8:207–217. doi:10.1038/nrmicro2298.

545 Terciolo C., Maresca M., Pinton P., Oswald I.P. 2018. 'Review article: Role of satiety
546 hormones in anorexia induction by Trichothecene mycotoxins', *Food Chem. Toxicol.*, 121:701–
547 714. doi:10.1016/j.fct.2018.09.034.

548 Theumer M.G., Henneb Y., Khoury L., Snini S.P., Tadriss S., Canlet C., Puel O., Oswald
549 I.P., Audebert M. 2018. 'Genotoxicity of aflatoxins and their precursors in human cells',
550 *Toxicol Lett.*, 287:100-107. doi: 10.1016/j.toxlet.2018.02.007.

551 Tromnet S. and Oswald, E. 2018. 'Quantification of Colibactin-associated Genotoxicity
552 in HeLa Cells by In Cell Western (ICW) Using γ -H2AX as a Marker', *Bio Protoc.*, 8:e2771.
553 doi:10.21769/BioProtoc.2771.

554 Van Der Fels-Klerx H.J., Liu C., Battilani P. 2016. 'Modelling climate change impacts
555 on mycotoxin contamination', *World Mycotoxins J.*, 5:717 -726. doi:10.3920/WMJ2016.2066

556 Varga E., Wiesenberger G., Hametner C., Ward T.J., Dong Y., Schöfbeck D.,
557 McCormick S., Broz K., Stücker R., Schuhmacher R. *et al.* 2015. 'New tricks of an old enemy:
558 isolates of *Fusarium graminearum* produce a type A trichothecene mycotoxin', *Environ.*
559 *Microbiol.* 17:2588-600. doi: 10.1111/1462-2920.12718.

560 Varga E., Wiesenberger G., Woelflingseder L., Twaruschek K., Hametner C.,
561 Vaclaviková M., Malachová A., Marko D., Berthiller F., Adam G. 2018. 'Less-toxic
562 rearrangement products of NX-toxins are formed during storage and food processing', *Toxicol.*
563 *Lett.*, 284:205-212. doi: 10.1016/j.toxlet.2017.12.016.

564 Wang W., Zhu Y., Abraham N., Li X.Z., Kimber M., Zhou T. 2021. 'The Ribosome-
565 Binding Mode of Trichothecene Mycotoxins Rationalizes Their Structure—Activity
566 Relationships', *Int. J. Mol. Sci.*, 22:1604. doi:10.3390/ijms22041604.

567 Weaver G.A., Kurtz H.J., Bates F.Y., Mirocha C.J., Behrens J.C., Hagler W.M. 1981.
568 'Diacetoxyscirpenol toxicity in pigs'. *Res. Vet. Sci.*, 31:131-5. doi: 10.1016/S0034
569 5288(18)32480-9.

570 Wu Q., Dohnal V., Kuca K., Yuan Z. 2013. 'Trichothecenes: Structure-toxic activity
571 relationships', *Curr. Drug Metab.*, 14:641–660. doi: 10.2174/1389200211314060002.

572 Wyatt R.D., Hamilton P.B., Burmeister, H.R. 1973. 'The Effects of T-2 Toxin in Broiler
573 Chickens', *Poultry Science*, 52:1853-1859. doi:10.3382/ps.0521853.

574 Yang Y., Gharaibeh R.Z., Newsome R.C., Jobin C. 2020. ‘Amending microbiota by
575 targeting intestinal inflammation with TNF blockade attenuates development of colorectal
576 cancer’, *Nat Cancer.*, 7:723-734. doi: 10.1038/s43018-020-0078-7.

577 Zhou H.R., He K., Landgraf J., Pan X., Pestka J.J. 2014. ‘Direct Activation of
578 Ribosome-Associated Double-Stranded RNA-Dependent Protein Kinase (PKR) by
579 Deoxynivalenol, Anisomycin and Ricin: A New Model for Ribotoxic Stress Response
580 Induction’, *Toxins*, 6: 3406–3425. doi:10.3390/toxins6123406.

581

582
583
584
585
586
587
588
589
590
591
592
593
594
595
596
597
598
599
600
601
602
603
604
605
606
607
608
609
610
611
612
613

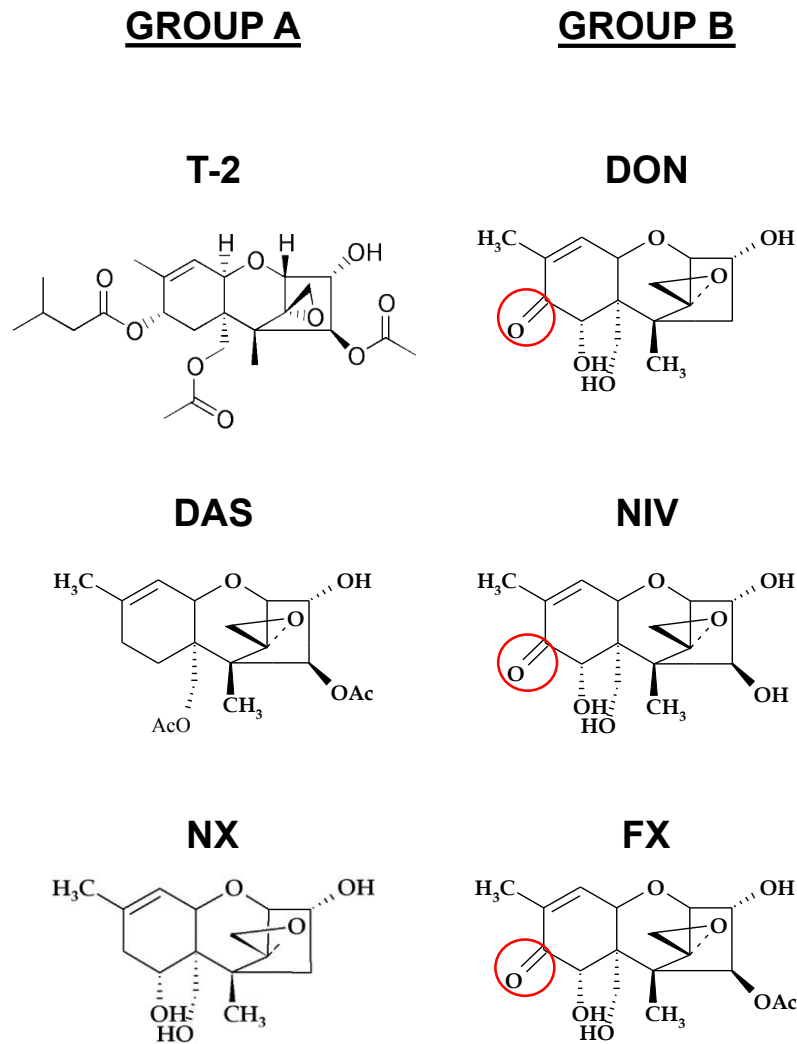


Figure 1: Chemical structures of trichothecenes. Dietary TCTs are classified in two main groups. Group A TCTs include T-2 toxin (T-2), diacetoxyscirpenol (DAS), and NX. Group B TCTs include deoxynivalenol (DON), nivalenol (NIV), and fusarenon-X (FX). Group A TCTs can be distinguished from group B TCTs by the presence of a C₈ keto-oxygen (circled in red).

614
 615
 616
 617
 618
 619
 620
 621
 622
 623
 624
 625
 626
 627
 628
 629
 630
 631
 632
 633
 634
 635
 636
 637
 638
 639
 640
 641
 642
 643
 644
 645
 646
 647

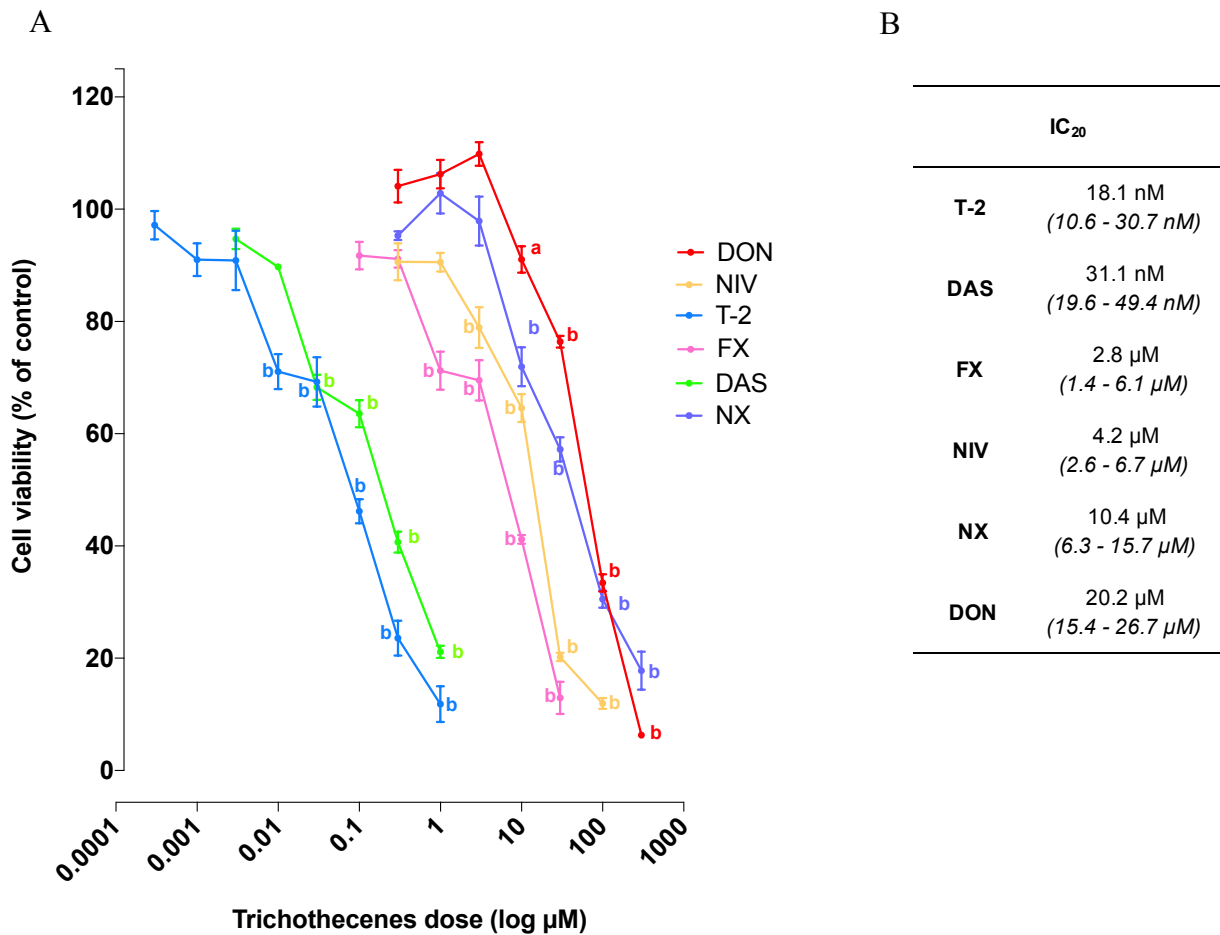
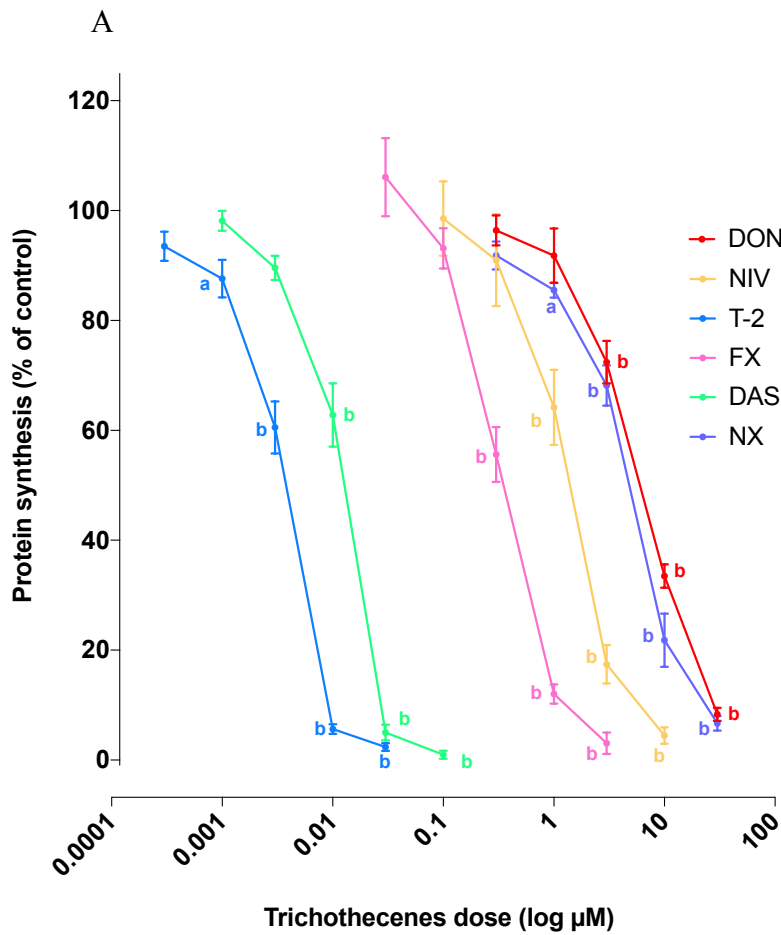


Figure 2: Trichothecenes induce dose-dependent cytotoxicity in cultured intestinal epithelial cells. A: Non-transformed rat intestinal epithelial IEC-6 cells were treated for 24 h with various concentrations of TCTs and then viability was assessed by measuring ATP levels. Data are expressed as mean ± SEM (3 to 6 independent experiments). P-values were calculated using one-way ANOVA with Bonferroni's multiple comparison, a: p<0.01; b: p<0.0001: B: Concentrations that inhibited cell viability by 20% (IC₂₀) for each trichothecene were calculated using the data presented in panel A. 95% confidence intervals are shown in italics.

648
 649
 650
 651
 652
 653
 654
 655
 656
 657
 658
 659
 660
 661
 662
 663
 664
 665
 666
 667
 668
 669
 670
 671
 672
 673
 674
 675
 676

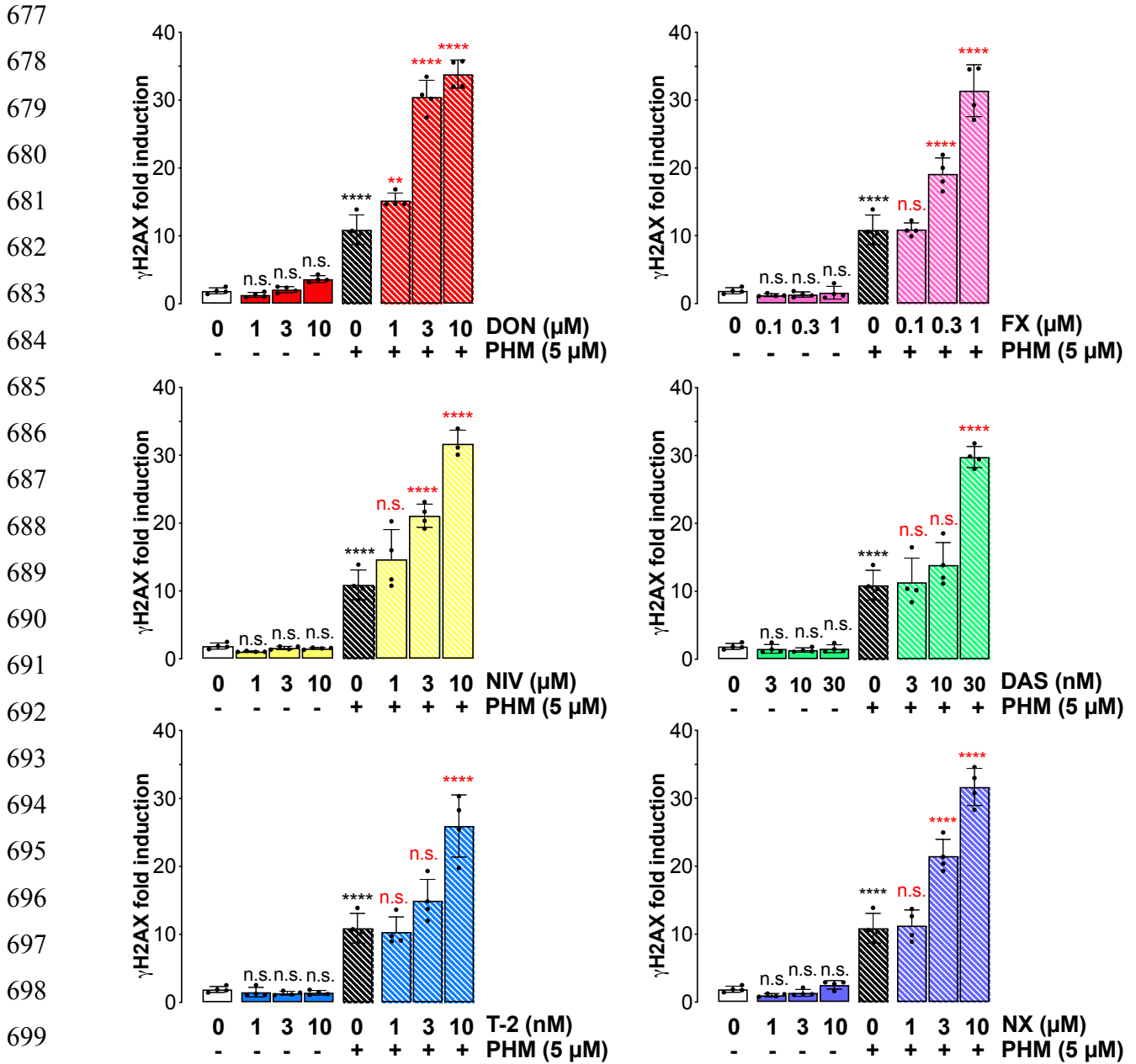


B

20% PSI level	
T-2	1.9 nM <i>(1.6 - 2.3 nM)</i>
DAS	6 nM <i>(5 - 7 nM)</i>
FX	0.15 μM <i>(0.12 - 0.19 μM)</i>
NIV	0.6 μM <i>(0.4 - 0.9 μM)</i>
NX	2.5 μM <i>(2.0 - 3.1 μM)</i>
DON	2.9 μM <i>(2.2 - 3.9 μM)</i>

Figure 3: Trichothecenes induce dose-dependent ribotoxicity in cultured intestinal epithelial cells. A: IEC-6 cells were treated for 4 h with different concentrations of TCTs and then the cells were treated for 30 min with puromycin, a protein translation marker. Incorporation of puromycin into newly synthesized peptides was quantified with an anti-puromycin antibody by In-Cell-Western. All the data are expressed as mean ± SEM (4 independent experiments). Values that are significantly different compared to the vehicle control are indicated a: p<0.01; b: p<0.0001: B: Concentrations that inhibited the protein synthesis by 20% (20% PSI) were calculated using the data presented in panel A. 95% confidence intervals are shown in italics.

A



B

No effect dose

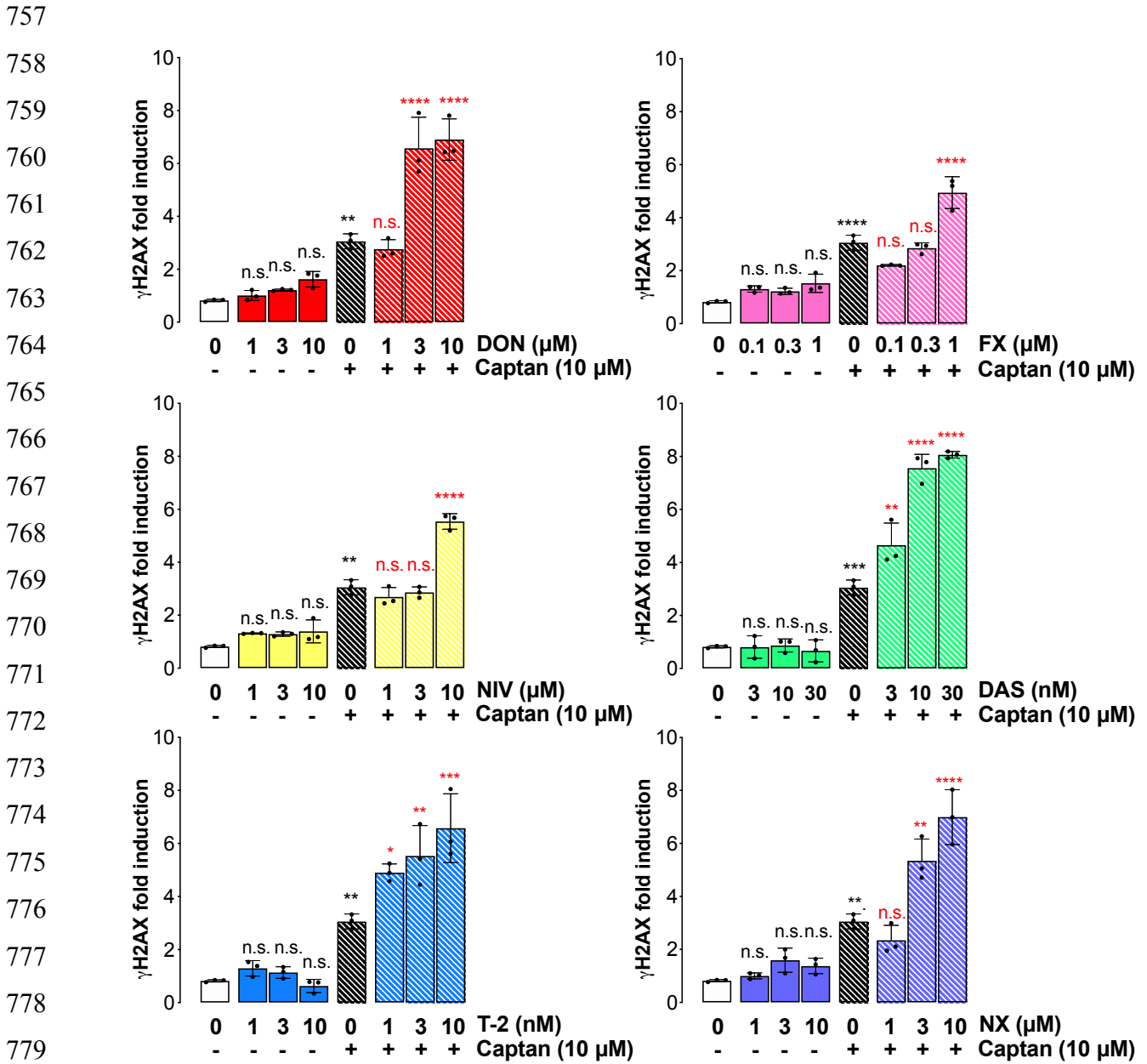
T-2	DAS	FX	NIV	DON	NX
3 nM	10 nM	0.1 μ M	1 μ M	< 1 μ M	1 μ M

710

711 **Figure 4: Trichothecenes exacerbate the genotoxicity induced by the DNA-damaging drug**
712 **phleomycin in a dose-dependent manner.** A: IEC-6 cells were co-treated for 4 h with 5 μ M
713 phleomycin (PHM) and increasing doses of DON (red), NIV (yellow), T-2 (blue), FX (pink), DAS
714 (green), or NX (purple). Then, DNA damage was measured by quantification of H2AX
715 phosphorylation by In-Cell-Western. All data are expressed as mean \pm SEM (4 independent
716 experiments). P-values were calculated using a one-way ANOVA with Bonferroni's multiple
717 comparison. Values that are significantly different compared to vehicle are indicated by black
718 asterisks, and values that are significantly different from infected cells without TCT are indicated
719 by red asterisks. *:p<0.1; **: p< 0.01; ***: p<0.001, ****: p< 0.0001, n.s. : not significant. B: No
720 exacerbation doses for each TCT were defined from data in panel A.

721
722
723
724
725
726
727
728
729
730
731
732
733
734
735
736
737
738
739
740
741
742
743
744
745
746
747
748
749
750
751
752
753
754
755

756 A



781 B

No effect dose					
T-2	DAS	FX	NIV	DON	NX
< 1 nM	< 3 nM	0.3 μ M	3 μ M	1 μ M	1 μ M

789 **Figure 5: Trichothecenes exacerbate the genotoxicity induced by the fungicide captan in a**
790 **dose-dependent manner.** A: IEC-6 cells were co-treated for 4 h with 10 μ M captan and increasing
791 doses of DON (red), NIV (yellow), T-2 (blue), FX (pink), DAS (green), or NX (purple). Then, DNA
792 damage was measured by quantification of H2AX phosphorylation by In-Cell-Western. All data are
793 expressed as mean \pm SEM (3 independent experiments). P-values were calculated using one-way
794 ANOVA with Bonferroni's multiple comparison. Values that are significantly different compared
795 to vehicle are indicated by black asterisks, and values that are significantly different from infected
796 cells without TCT are indicated by red asterisks. *:p<0.1; **: p< 0.01; ***: p<0.001, ****: p<
797 0.0001, n.s.: not significant. B: No exacerbation dose for each TCT was defined from data in panel
798 A.

799

800

801

802

803

804

805

806

807

808

809

810

811

812

813

814

815

816

817

818

819

820

821

822

823 A

824

825

826

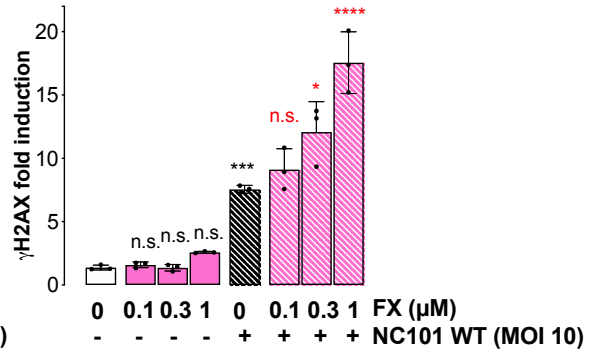
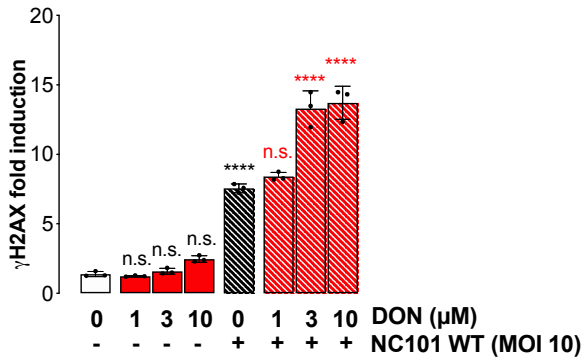
827

828

829

830

831



832

833

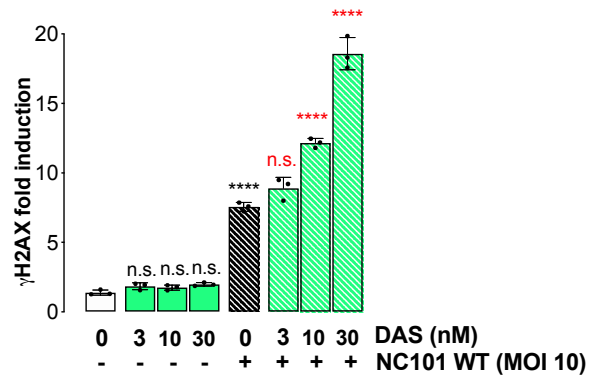
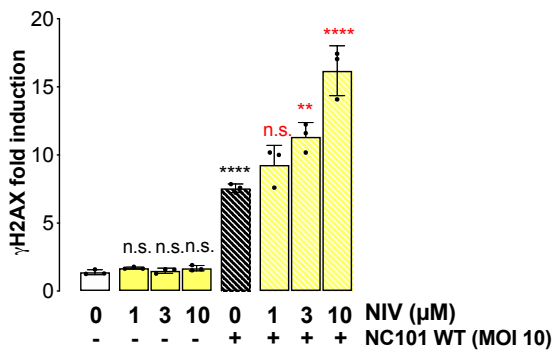
834

835

836

837

838



839

840

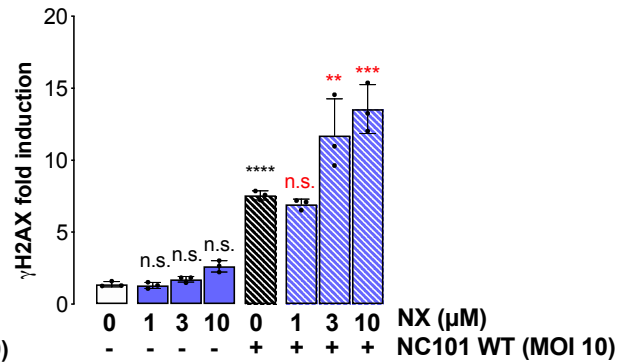
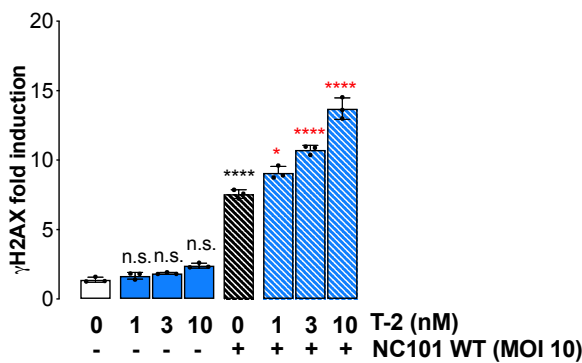
841

842

843

844

845



846

847

848

B

No effect dose

T-2	DAS	FX	NIV	DON	NX
< 1 nM	3 nM	0.1 μM	0.3 μM	1 μM	1 μM

855

856

857 **Figure 6: Trichothecenes exacerbate the genotoxicity induced by the bacterial genotoxin**
858 **colibactin in a dose-dependent manner.** A: IEC-6 cells were infected 4 h with live colibactin-
859 producing *E. coli* strain NC101 (multiplicity of infection of 10 bacteria per cell) with increasing
860 doses of DON (red), NIV (yellow), T-2 (blue), FX (pink), DAS (green), or NX (purple). Cells were
861 washed to remove bacteria and further incubated with the TCTs for 4 h. Then, DNA damage was
862 measured by quantification of H2AX phosphorylation by In-Cell-Western. All data are expressed
863 as mean \pm SEM (3 independent experiments). P-values were calculated using one-way ANOVA
864 with Bonferroni's multiple comparison. Values that are significantly different compared to vehicle
865 are indicated by black asterisks, and values that are significantly different from infected cells
866 without TCT are indicated by red asterisks. *: $p < 0.1$; **: $p < 0.01$; ***: $p < 0.001$, ****: $p < 0.0001$,
867 n.s.: not significant. B: No exacerbation doses for each TCT were defined from data shown in figure
868 6A.

869

870

871

872

873

874

875

876

877

878

879

880

881

882

883

884

885

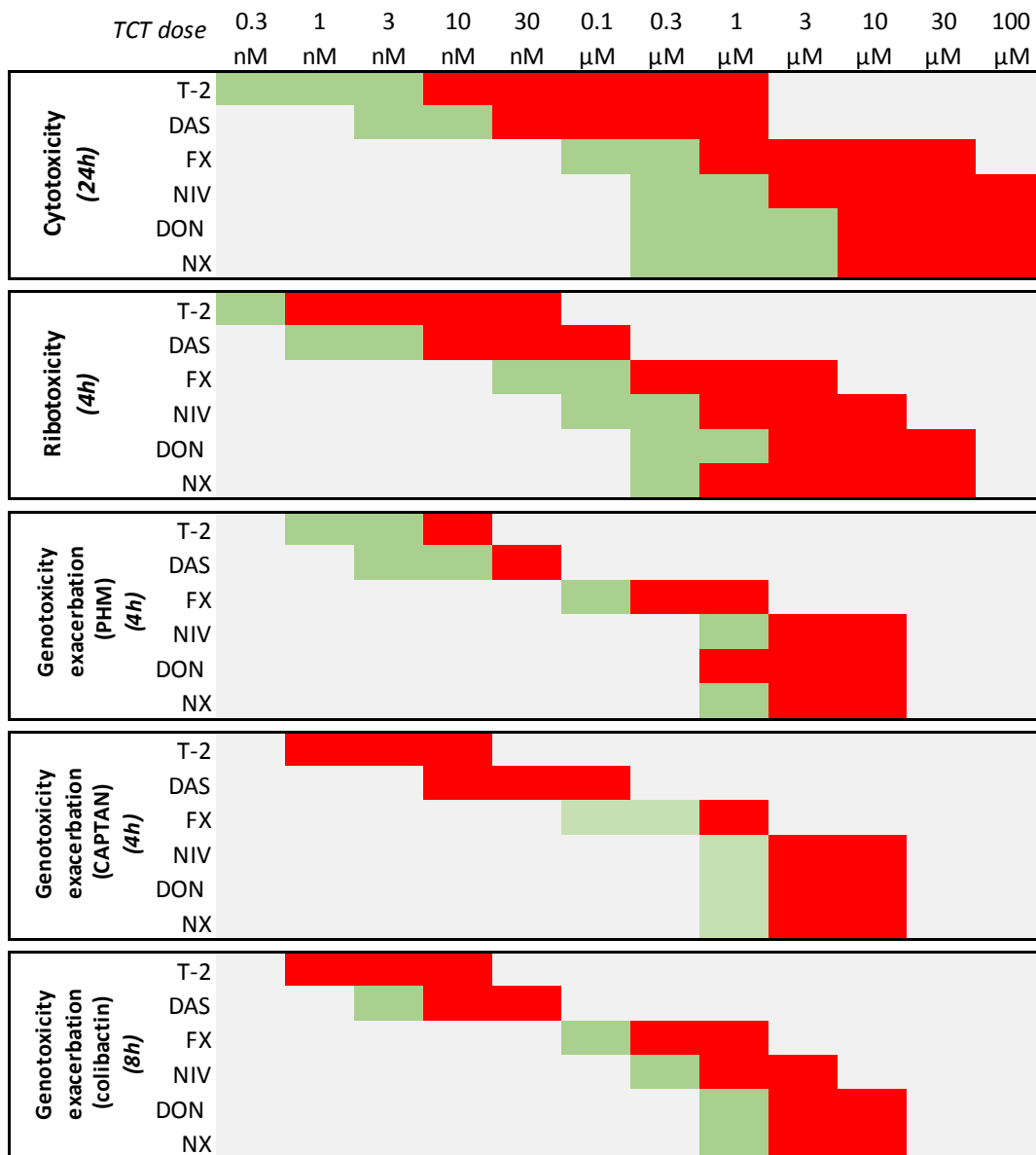
886

887

888

889

890



892

893

894 **Table 1: Trichothecenes classification for cytotoxicity, ribotoxicity, and capacity to**
 895 **exacerbate the genotoxicity.** Green boxes: doses inducing no significant cytotoxicity,
 896 ribotoxicity or genotoxicity exacerbation. Red boxes: doses inducing significant cytotoxicity,
 897 ribotoxicity or genotoxicity exacerbation.

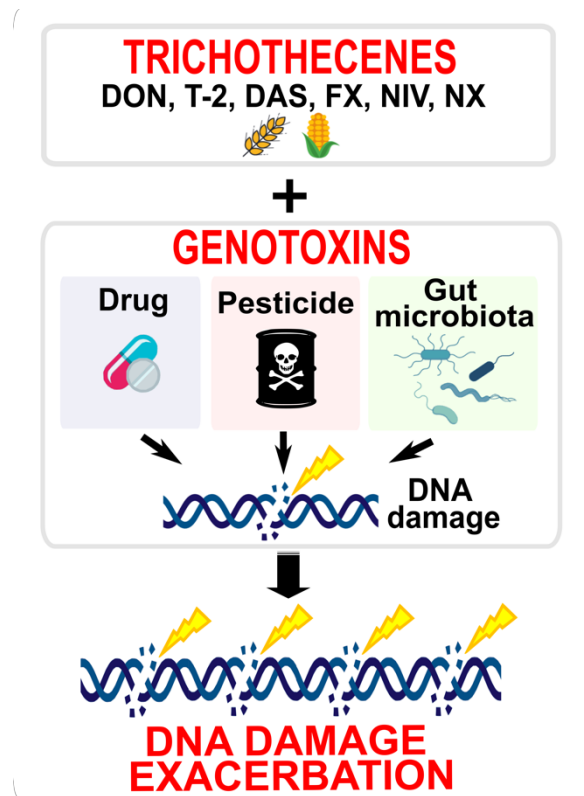
898

899

HIGHLIGHTS

- A novel effect of trichothecenes (TCTs) has been identified
- TCTs exacerbate genotoxicity
- Six type A or type B TCTs display this effect
- This effect is observed with a drug, a pesticide, and a toxin produced by microbiota
- For genotoxicity exacerbation, TCTs are classified: T-2>DAS>FX>NIV≥DON≥NX

GRAPHICAL ABSTRACT



1 **Supplementary material for**

2 **“A novel toxic effect of trichothecenes: the exacerbation of genotoxicity”**

3
4 Marion Garofalo^{a,b}, Delphine Payros^{a,b}, Marie Penary^b, Eric Oswald^{b,c}, Jean-Philippe
5 Nougayrède^{b*}, Isabelle P. Oswald^{a*}.

6
7 ^aToxalim (Research Centre in Food Toxicology), Université de Toulouse, INRAE, ENVT, INP-
8 Purpan, UPS, Toulouse, France

9 ^bIRSD, Université de Toulouse, INSERM, INRAE, ENVT, UPS, Toulouse, France

10 ^cCHU Toulouse, Hôpital Purpan, Service de Bactériologie-Hygiène, Toulouse, France

11
12 *Corresponding authors: isabelle.oswald@inrae.fr; jean-philippe.nougayrede@inrae.fr

13 Keywords: trichothecenes; genotoxins; colibactin; DNA damage.

14
15 **Supplementary methods 1:**

16
17 ***In vitro* crosslinking assay and bacterial load analysis.** To examine colibactin production by
18 the bacteria, a DNA crosslinking assay was performed as previously described (Bossuet-Greif
19 *et al.*, 2018). Briefly, 400 ng linear DNA was exposed to 1.5×10^6 bacteria in 100 μ l infection
20 medium in the presence of TCTs or DMSO vehicle. After 4 h at 37°C, bacteria were pelleted,
21 plated on LB agar plates, and enumerated. The DNA was purified from the culture supernatant
22 using the Qiagen QIAquick PCR kit (Qiagen, Hilden, Germany). Purified DNA was loaded on
23 a denaturing agarose gel (pH 8) and electrophoresis was carried for 45 min at 25V followed by
24 2 h 30 min at 50V. After gel neutralization, DNA was stained with Gel Red (Biotium, San
25 Francisco, USA) and visualized in a Bio-Rad Chemidoc XRS system. The percentage of
26 crosslinked DNA was quantified by using the FIJI software (<https://imagej.net/Fiji>).

27
28
29
30
31
32
33
34

35
36
37
38
39
40
41
42
43
44
45
46
47
48
49
50
51
52
53
54
55
56
57
58
59
60
61
62
63
64
65
66
67
68

DNA quantification (% of control cells)					
	No genotoxin (4h)	No genotoxin (8h)	Phleomycin (5 μ M) (4h)	Captan (10 μ M) (4h)	NC101 WT (MOI 10) (8h)
Control (vehicle)	100	100	98.8 \pm 1.6	90.1 \pm 1.3	105.1 \pm 2.8
DON (10 μM)	83.7 \pm 5.8	87.6 \pm 6.9	82.4 \pm 13.2	99.8 \pm 12.5	91.6 \pm 8.5
T-2 (10 nM)	86.2 \pm 6.6	95.5 \pm 2.0	97.7 \pm 17.9	107.6 \pm 7.8	112.8 \pm 3.7
DAS (30 nM)	92.2 \pm 12.8	94.2 \pm 6.2	104.1 \pm 11.6	108.8 \pm 3.04	111.4 \pm 3.7
NIV (3 μM)	100.6 \pm 5.4	103.9 \pm 8.4	100.1 \pm 6.2	114.7 \pm 4.3	109.8 \pm 7.4
FX (1 μM)	101.8 \pm 3.4	103.7 \pm 1.0	90.5 \pm 5.2	107.9 \pm 12.0	107.0 \pm 2.7
NX (10 μM)	85.9 \pm 6.9	97.4 \pm 2.4	77.4 \pm 6.8	85.5 \pm 4.1	79.1 \pm 0.9

Table S1: The genotoxicity exacerbation induced by trichothecenes is not associated with cytotoxicity. DNA in the cells was calculated from RedDot2 DNA staining using the In-Cell-Western method. Values were obtained after normalization from untreated cells considered as 100%.

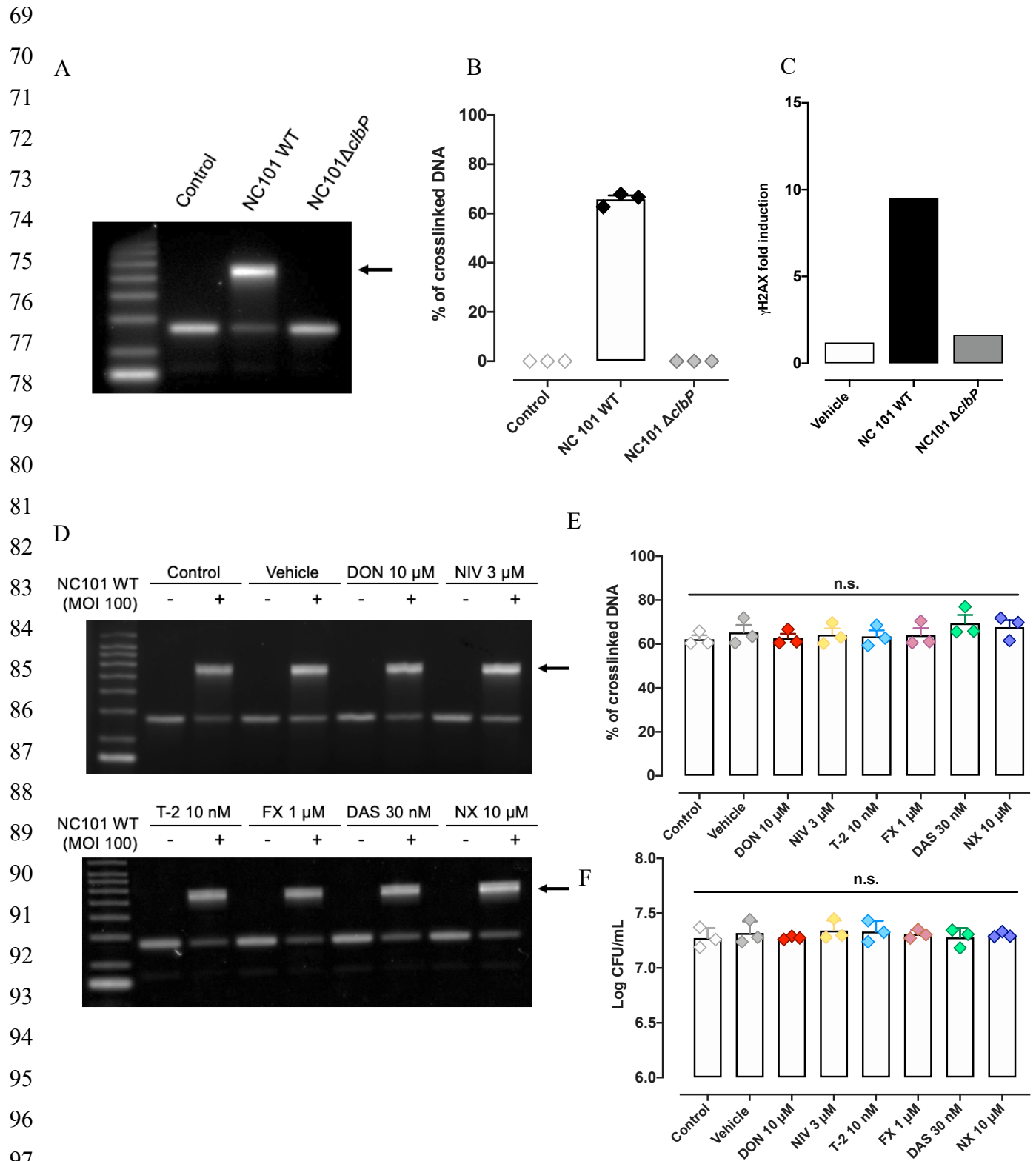
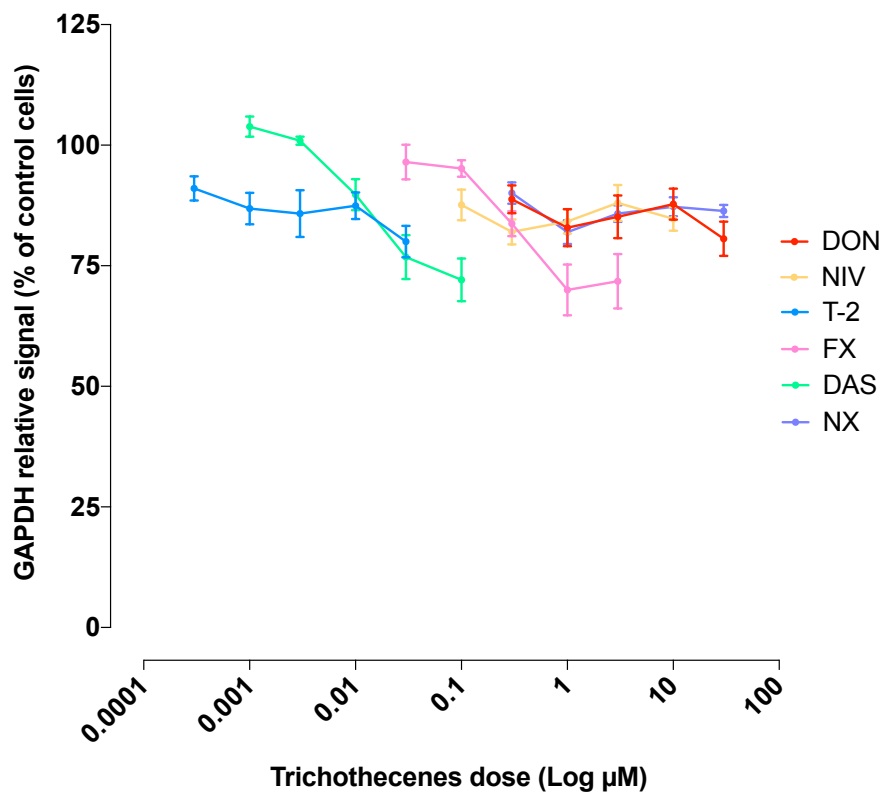


Figure S1: Trichothecenes does not impact colibactin production and bacterial growth.

A, B: *E. coli* NC101 WT or $\Delta clbP$ (MOI 100) were grown for 3.5 h, and then linearized DNA was added and incubated for 30 min. DNA was purified and analysed by denaturing gel electrophoresis, and the percentage of crosslinked DNA (arrow) was quantified by image

103 analysis. C: Non-transformed rat intestinal epithelial IEC-6 cells were infected for 4 h with the
104 producing-colibactin *E. coli* strain NC101 WT or to the colibactin-deficient strain NC101 $\Delta clbP$
105 (MOI 10). Then, H2AX phosphorylation levels were quantified by In-Cell-Western. D, E:
106 colibactin production was measured as in panel A in presence of TCTs. F: after the interaction
107 between bacteria TCT and DNA, the bacteria were counted by serial dilution and plating. After
108 an overnight incubation, Colony Forming Units (CFU) were enumerated. All the data are
109 expressed as mean \pm SEM (3 independent experiments). All P-values are calculated using one-way
110 ANOVA with Bonferroni's multiple comparison. n.s: not significant.



129 **Figure S2:** Non-transformed rat intestinal epithelial IEC-6 cells were treated for 4 hours with
130 various concentrations of DON (red), NIV (yellow), T-2 (blue), FX (pink), DAS (green), or NX
131 (purple). GAPDH levels were measured with an anti-GAPDH antibody by In-Cell-Western. All the
132 data are expressed as mean \pm SEM (4 independent experiments).

133